Atmos. Chem. Phys., 26, 6727–6739, 2026
https://doi.org/10.5194/acp-26-6727-2026

Atmospheric Chemistry and Physics
Open Access
EGU

Research article

Organic amine weakens chloride depletion in coastal atmosphere

Aijing Song[1], Kun Li[1], Zhaomin Yang[1], Li Xu[2], Narcisse Tsona Tchinda[1], and Lin Du[1,2,3]

[1]Qingdao Key Laboratory for Prevention and Control of Atmospheric Pollution in Coastal Cities, Environment Research Institute, Shandong University, Qingdao 266237, China
[2]School of Environmental Science and Engineering, Shandong University, Qingdao 266237, China
[3]State Key Laboratory of Microbial Technology, Shandong University, Qingdao 266237, China

Correspondence: Lin Du (lindu@sdu.edu.cn)

Received: 14 January 2026 – Discussion started: 2 February 2026
Revised: 23 April 2026 – Accepted: 9 May 2026 – Published: 19 May 2026

Abstract. Chloride depletion from sea salt aerosols (SSA) is frequently observed in polluted coastal regions, and despite they severely impact air quality and human health, the influencing mechanism of alkaline species in this phenomenon remains incompletely understood. Here, we conducted laboratory experiments to investigate the effect of alkaline species including NH_3 and an organic amine (dimethylamine, DMA) on chloride depletion and the subsequent formation of organic chlorinated compounds. Results showed that alkaline species could weaken chloride depletion caused by acidic gases, mainly due to acid-base neutralization. Specifically, chloride depletion in the presence of NO_x decreased from 20.1 % to 15.8 % when NH_3 concentration increased from 100 to 300 ppb. Chloride depletion also decreased from 18.6 % to 13.5 % with DMA concentration increasing from 50 to 150 ppb. The weakening effect of DMA on chloride depletion is more pronounced than that of NH_3, primarily DMA stronger alkalinity and nucleation ability. These alkaline species exhibit a stronger reduction of chloride depletion in the presence of SO_2 than in the presence of NO_x. The detection of organic chlorinated products, formed via active chlorine-induced oxidation, is consistent with the role of alkaline species in weakening chloride depletion, which subsequently results in the reduction of active chlorine. These findings suggest that alkaline species, more specifically organic amines, are significant factors influencing chloride depletion in the coastal atmosphere, further improving our understanding of this phenomenon.

1 Introduction

Sea salt aerosols (SSA), primarily composed of sodium chloride, are abundant in coastal areas and play a key role in cloud nucleation with high light scattering efficiency (Zhang and Chan, 2023; Zhou et al., 2025). Chloride depletion, referred to as the removal of chloride ions from SSA and frequently observed in the coastal atmosphere (Bian et al., 2014; Duan et al., 2024; Su et al., 2022), accelerates their aging process of SSA, profoundly influencing visibility, global climate and the earth-atmosphere radiative balance (Ghosh et al., 2020; Edwards et al., 2024; Su et al., 2022). This process also affects the atmospheric oxidation capacity by producing Cl_2, HCl, $Cl^{\bullet}$, and other reactive species (Hoffmann et al., 2019; Chen et al., 2024b; Dai et al., 2025). However, significant discrepancies exist between field observations and model predictions of chloride depletion with an average absolute difference of 20 % (Nolte et al., 2008, 2015; Su et al., 2022), highlighting the need for a deeper understanding of its underlying mechanisms.

Alkaline species such as NH_3 and organic amines have been suspected to affect chloride depletion (Su et al., 2022). Gaseous ammonia (NH_3), the most abundant alkaline species in the atmosphere, plays an important role in the formation of atmospheric particles (Behera et al., 2013; Lan et al., 2024; Wang et al., 2020). A field study found a relatively low level of chloride depletion in the Antarctic winter, and the large amount of ammonia emitted by penguins has been hypothesized to be responsible for this phenomenon (Rankin and

Wolff, 2003). Dimethylamine (DMA, $(CH_3)_2NH$), a predominant organic amine in the atmosphere, has a stronger alkalinity than ammonia and could compete with ammonia in reactions with acidic species, despite its atmospheric concentration being much lower than that of ammonia (Chen et al., 2022; Xie et al., 2018; Liu et al., 2024a). However, to the best of our knowledge, there is currently no experimental evidence illustrating the role of alkaline species in chloride depletion. The influence of organic amines remains overlooked in model predictions (Nolte et al., 2015), highlighting a critical gap for accurately predicting chloride depletion in amine-rich coastal or agricultural-marine interfaces.

Organic chlorinated compounds are important indicators of chloride depletion. They can be formed from the oxidation of volatile organic compounds (VOCs) by reactive chlorine species (e.g., $Cl^{\bullet}$, $Cl_2^{\bullet-}$, etc.) generated during the chloride depletion process (Zhang and Chan, 2023; Wennberg et al., 2018; Wang et al., 2022b). Once formed, some organic chlorinated compounds with low volatility can partition into the particle phase, contributing to the formation of secondary organic aerosols (SOA). For example, it is estimated that organic chlorinated compounds can contribute up to 15 % of the total SOA in polluted areas with sufficient chlorine and VOC emissions (Liu et al., 2024c). Organic chlorinated compounds have been observed during chloride depletion in our previous study in the presence of isoprene (Song et al., 2025), an important biogenic VOC emitted from ocean and terrestrial plants (Yu and Li, 2021; Zhang et al., 2025; Zou et al., 2023). Understanding the formation of organic chlorinated compounds would not only help elucidating the influence of alkaline species on chloride depletion but also provide significant implications for the chlorine cycle.

To investigate the roles of alkaline species, including NH_3 and DMA, in chloride depletion, experiments on reactions involving SSA particles, alkaline species, acidic gases, and/or isoprene were conducted in a chamber. We characterized the changes in chloride depletion and further analyzed the subsequent formation of corresponding organic chlorinated compounds to explore the reasons for their changes. This study provides a comprehensive understanding of chloride depletion from SSA, which may be crucial for more accurately predicting this phenomenon in coastal atmospheres.

2 Materials and methods

2.1 Chamber experiments

To study the effect of alkaline species on chloride depletion, three groups of experiments were designed: NaCl particles + NH_3 / DMA (control experiments), NaCl particles + H_2O_2 + NO_x / SO_2 + NH_3 / DMA, and NaCl particles + H_2O_2 + isoprene + NO_x / SO_2 + NH_3 / DMA. Here, the shifting ratios of ammonia to DMA are in the range 0.67–6, which falls within the ranges observed in diverse coastal environments (0.1–110) (Smith et al., 2007; Chen et al., 2022; Berner and David Felix, 2020; Liu et al., 2022, 2024b, 2023; Du et al., 2021). Although the initial concentrations of alkaline species used in the experiments were higher than the ambient levels, this consideration was necessary for laboratory experiments within a short time scale to tackle their influence on chloride depletion. Details of experimental conditions are provided in Table 1. All experiments were conducted in a 1.5 m^3 indoor chamber consisting of 60 µm Teflon film within a temperature-controlled environment, surrounded by black light lamps (F40BLB, GE) with the center irradiation wavelength of 365 nm as the light source. The chamber was equipped with a set of online instruments for measuring physical and chemical parameters. The concentration of aerosol particles was measured using a scanning mobility particle sizer (SMPS, Grimm, Germany), which is composed of a differential mobility analyzer (DMA, 55-L, Grimm, Germany) and a condensation particle counter (CPC, 5416, Grimm, Germany). The concentrations of NO_x and isoprene in the chamber were monitored using a NO–NO_2–NO_x analyzer (Model 42i, Thermo Scientific, USA) and a gas chromatograph coupled with a flame ionization detector (GC-FID 7890B, Agilent Technologies, USA). H_2O_2 acted as the source of OH radicals. The initial concentrations of other substances (H_2O_2, alkaline gases, etc.) were calculated based on the chamber volume and the injection volume.

The chamber was thoroughly cleaned using O_3 and purified air, and exposed to UV lamps for at least 12 h before each experiment. Relative humidity (RH) in the chamber was adjusted by the proportion of dry and wet air. Subsequently, SSA particles produced by atomizing NaCl solution with an atomizer (Model 3076, TSI, USA) were introduced into the chamber. Based on the experimental design, known volumes of other reactants (i.e., H_2O_2 (Aladdin, 30 wt % in H_2O), inorganic gases (NH_3, NO, etc) (Qingdao Deyi Gas Company, 500 ppm balanced in N_2), DMA (Aladdin, 40 wt % in H_2O), and isoprene (Macklin, > 99 %)) were introduced into the chamber. After the reactants were adequately mixed for 20 min, the black light lamps were turned on to initiate the reaction. The experiment lasted for two hours, after which aerosol particles generated during the experiment were collected onto quartz filters and 47 mm polytetrafluoroethylene (PTFE) filters and stored at −20 °C until offline analysis.

2.2 Particle analysis

The concentrations of inorganic ions were measured by ion chromatography (IC, Dionex ICS-600, Thermo Scientific, USA). Aerosol particles collected on the quartz filters were first extracted in 5 mL of ultrapure water (Milli-Q, Millipore, France) by ice sonication for 45 min. The extract was then filtered through a 0.22 µm polyethersulfone syringe filter and injected into the ion chromatography instrument via a six-way valve with a 250 µL loop. The separation of anions and cations was achieved using a Dionex IonPac AS19 column (4 × 250 mm) with an AG19 guard column (4 × 50 mm,

Table 1. Summary of experimental conditions and results.

Experiment[a]	[Isoprene]$_0$ (ppb)	[H_2O_2]$_0$ (ppm)	[NO_x]$_0$ (ppb)	[SO_2]$_0$ (ppb)	[NH_3]$_0$ (ppb)	[DMA]$_0$ (ppb)	RH (%)	T (°C)	Cl^-/Na^+ (mM / mM)[c]
C.1					100		72	20	0.989 ± 0.019
C.2						100	71	20	0.994 ± 0.020
N.1		4	141				69	23	0.755 ± 0.015
NA.1		4	138		100		69	21	0.798 ± 0.016
NA.2		4	139		200		72	21	0.822 ± 0.017
NA.3		4	139		300		72	20	0.841 ± 0.017
ND.1		4	146			50	69	21	0.813 ± 0.017
ND.2		4	147			100	71	21	0.849 ± 0.017
ND.3		4	141			150	71	22	0.864 ± 0.018
S.1		4		300			67	22	0.704 ± 0.009
SA.1		4		300	100		70	23	0.825 ± 0.017
SA.2		4		300	200		70	23	0.839 ± 0.017
SA.3		4		300	300		69	23	0.849 ± 0.017
SD.1		4		300		50	70	22	0.851 ± 0.017
SD.2		4		300		100	71	22	0.865 ± 0.018
SD.3		4		300		150	70	23	0.878 ± 0.018
IN.1[b]	667	4	150				72	20	0.770 ± 0.016
INA.1[b]	621	4	140		100		71	22	0.784 ± 0.016
INA.2	604	4	161		300		69	23	0.791 ± 0.016
IND.1[b]	601	4	152			100	68	22	0.814 ± 0.017
IND.2	668	4	146			150	70	20	0.866 ± 0.018
IS.1[b]	776	4		300			68	20	0.655 ± 0.008
ISA.1[b]	604	4		300	100		70	20	0.790 ± 0.016
ISA.2	601	4		300	300		71	21	0.800 ± 0.016
ISD.1[b]	629	4		300		100	70	21	0.897 ± 0.018
ISD.2	594	4		300		150	69	22	0.961 ± 0.020

[a] Abbreviations used in experimental codes correspond to the reactants introduced into the chamber. "N", "S", "A", "D", and "I" stand for NO_x, SO_2, NH_3, DMA, and isoprene, respectively. C.1 and C.2 are control experiments. [b] Experiments were repeated to collect aerosol particles for composition measurement by UPLC/ESI-HR-Q-TOFMS. [c] Errors in Cl^-/Na^+ were calculated by error propagation considering Cl^- and Na^+ errors derived from their IC calibration curve.

Dionex Ionpac) for anions, and a Dionex IonPac CS12A column (4 × 250 mm) with a CG12A guard column (4 × 50 mm, Dionex Ionpac) for cations. A 20 mM potassium hydroxide solution was used as the anionic eluent, while a 20 mM methanesulfonic acid solution was employed for cationic elution. The flow rate for both eluents was maintained at 1 mL min^{-1}. The degree of chloride depletion was characterized by the mole ratios of Cl^-/Na^+. The Cl^-/Na^+ value for fresh SSA is around 0.999, while lower Cl^-/Na^+ ratios in SSA indicate the occurrence of chloride depletion.

The formation of organic chlorinated compounds was characterized using ultra-high performance liquid chromatography (UPLC, UltiMate 3000, Thermo Scientific, USA) coupled with electrospray ionization high-resolution quadrupole time-of-flight mass spectrometer (ESI-HR-Q-TOF-MS, Bruker Impact HD, Germany). Prior to measurements, aerosol particles collected on PTFE filters were extracted twice using 5 mL methanol (Optima® LC/MS grade, Fisher Scientific, USA) by sonication in an ice bath for 30 min. The extract was filtered through a PTFE syringe filter (0.22 µm) to remove impurities, and then concentrated under a gentle nitrogen gas (99.999 %, Qingdao Deyi Gas Company). The dried extract was reconstituted in 200 µL of a 1 : 1 ($v : v$) mixture of methanol and ultrapure water containing 0.1 % formic acid (Optima® LC/MS grade, Fisher Scientific, USA). Sample extracts (10 µL) were analyzed using an Atlantis T3 C18 column (100 Å, 3 µm particle size, 2.1 mm × 150 mm, Waters, USA). The mobile phase comprised 0.1 % formic acid in ultrapure water (A) and 0.1 % formic acid in methanol (B). A 60 min gradient elution with a flow of 200 µL min^{-1} was performed as follows: B initially maintained at 3 % for the first 3 min, gradually increased to 50 % from 3 to 25 min, and then rose to 90 % from 25 to 43 min. The fraction of B was reduced back to 3 % between 43 and 48 min, and maintained at 3 % until 60 min to re-equilibrate the column.

Mass spectrometric data were analyzed with Bruker Compass Data Analysis version 4.2 Build 383.1 soft-

ware. The molecular formulas of organic chlorinated compounds were assigned as $C_{2–40}H_{2–80}O_{0–40}N_{0–3}S_{0–2}Cl_{1–2}$ within a ±5 ppm mass tolerance, with restrictive conditions applied to exclude unreasonable formulas: $1 \le H/C \le 3$, $0.2 \le O/C < 1.5$, $0 \le N/C \le 0.5$, $0 \le S/C \le 1$, $S/O \le 0.25$, $0 <$ double bond equivalent (DBE) / $C < 1$. The organic chlorinated compounds were reliably identified based on their isotopic mass and intensity, but the identified formulas containing isotopes (e.g., ^{13}C, ^{18}O, ^{34}S, and ^{37}Cl) were not further discussed. The carbon oxidation state (OS_C) and DBE of the assigned molecular formula ($C_cH_hO_oN_nS_sCl_j$) were calculated as follows:

$$\mathrm{DBE} = 1 + \frac{2c - (h + j) + n}{2} \quad (1)$$

$$\mathrm{OS_C} \approx 2 \times \frac{\mathrm{O}}{\mathrm{C}} - \frac{\mathrm{H}}{\mathrm{C}} \quad (2)$$

The toxicity of identified organic chlorinated compounds was analyzed based on their possible chemical structures using Toxicity Estimation Software Tool (T.E.S.T., V.5.1.2, USEPA) to estimate their oral rat pLD_{50} ($-\log_{10}$(pred), mol kg^{-1}), developmental toxicity, and mutagenicity.

2.3 Box model

The Framework for 0-D Atmospheric Modeling (F0AM) (Wolfe et al., 2016) was used to further investigate the impact of alkaline species on chloride depletion. The gas phase reactions used in this study were derived from the Master Chemical Mechanism (MCM) v3.3.1 (http://mcm.york.ac.uk/, last access: 16 July 2025) (Jenkin et al., 2015). Based on the heterogeneous reactions integrated in our previous work (Song et al., 2026), we further incorporated the acid-base neutralization reactions into the mechanism, with a rate constant of 2.64×10^{-16} cm^3 molec.$^{-1}$ s^{-1} for the reaction between NH_3 and HNO_3 (Behera and Sharma, 2012). The initial conditions in the model were set to match those of the chamber experiments.

3 Results and discussion

3.1 Effects of NH_3 on chloride depletion

A series of experiments were designed with varying initial concentrations of alkaline species in the presence of acid gases, i.e., SO_2 and NO_x, to evaluate the effect of alkaline species on chloride depletion (Table 1). Although NH_3 addition induced no significant change in chloride depletion in the absence of SO_2 and NO_x (Exp. C.1), it could significantly hinder this process in their presence (Fig. 1a). For example, the mole ratios of Cl^-/Na^+ increased from 0.798 to 0.841 when the concentration of NH_3 raised from 100 to 300 ppb under constant NO_x (Exp.NA.1–NA.3), while this ratio was 0.755 when only NO_x was present (Exp.N.1). This corresponds to a reduction in chloride depletion from 20.1 % to 15.8 %. In these experiments, $NO_2 + OH$ or $N_2O_5 + H_2O$ reactions could lead to the formation of nitric acid (HNO_3), which can induce chloride depletion through the replacement reaction (Su et al., 2022; Xu et al., 2021). The suppressed chloride depletion by NH_3 can be attributed to the neutralization reaction between NH_3 and HNO_3 that generates NH_4NO_3 particles (Behera et al., 2013). Although NH_4NO_3 is unstable (Behera et al., 2013; Lan et al., 2024), ammonium ions were detected in these experiments. Furthermore, the time series of the HNO_3 and Cl radicals exposure were simulated using F0AM for Exp.N.1–NA.3 (Fig. S1 in the Supplement). The exposure of HNO_3 and Cl radicals decreased after NH_3 addition, further supporting the crucial role of the reaction between NH_3 and HNO_3 in reducing chloride depletion. As shown in Table S1 in the Supplement, the exposure of HNO_3 and Cl radicals also decreased after the addition of NH_3 (0–20 ppb), demonstrating that the observed mechanisms persist at near-ambient concentrations. In the presence of SO_2, the effect of NH_3 on reducing chloride depletion is even more pronounced. For example, the addition of 300 ppb NH_3 (Exp.SA.3) reduced SO_2-induced chloride depletion from 29.5 % (Exp.S.1) to 15.0 %. This can be explained by the generation of $(NH_4)_2SO_4$ via the reaction of NH_3 with sulfuric acid (H_2SO_4), which is produced from the oxidation of SO_2 by OH radicals (Lan et al., 2024; Behera et al., 2013). As shown in Fig. S2, ammonium ion was detected in Exp.SA.1–SA.3. Notably, the $H_2SO_4 + NH_3$ reaction is much more thermodynamical and kinetically favorable than the $HNO_3 + NH_3$ reaction (Behera et al., 2013). This may be the reason why the reduction in chloride depletion was more significant in experiments SA.1–SA.3 compared to experiments NA.1–NA.3. Our findings further support the hypothesis formulated from field studies that ammonia can reduce chloride depletion (Rankin and Wolff, 2003; Braun et al., 2017; Zhan et al., 2017; Chen et al., 2016; Yao et al., 2003; Ghosh et al., 2020).

Isoprene was further introduced into the experimental chamber with various initial NH_3 concentrations to study the combined effect of alkaline gases with isoprene and acidic gases (Fig. 1b). Similar to the above experiments without isoprene, NH_3 can reduce the chloride depletion caused by acidic gases, with a more pronounced weakening effect in the presence of SO_2. Notably, the addition of isoprene reduced the ability of NH_3 to weaken chloride depletion, resulting in its relative enhancement. For instance, chloride depletion was 20.8 % in the experiment with isoprene and NH_3 (Exp.INA.2), significantly higher than 15.8 % in the experiment without isoprene (Exp.NA.3). Slightly different values, namely 19.9 % and 15.0 % were observed in Exp.ISA.2 and Exp.SA.3, respectively, which can be attributed to the reaction of NH_3 with SOA constituents such as organic acids, or other species generated from the oxidation of isoprene to form nitrogen-containing organic compounds (Li et al., 2024; Wu et al., 2021; Wennberg et al., 2018; Bates et al.,

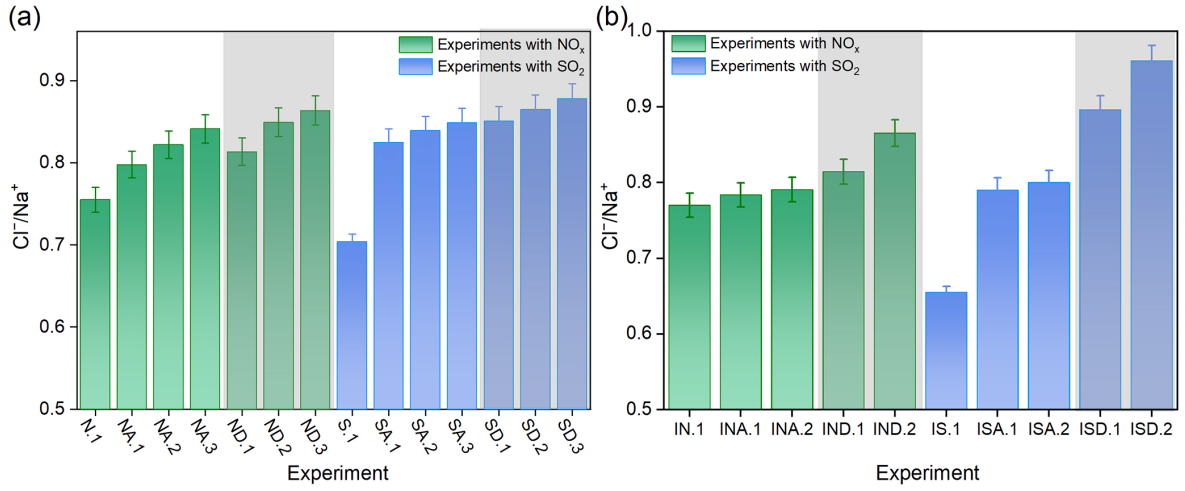

Figure 1. Dependences of Cl^-/Na^+ ratio on the concentrations of different alkaline species in the **(a)** absence and **(b)** presence of isoprene. The experiments with a grey background indicate the addition of DMA.

2023). This leads to reduced NH_3 for neutralizing acid-induced chloride depletion.

3.2 Effects of DMA on chloride depletion

DMA was introduced into the reaction system to investigate its influence on chloride depletion. Similar to NH_3, DMA also caused negligible chloride depletion in the absence of acidic gases (Exp.C.2, Table 1). In the presence of acidic gases, the weakening effect of chloride depletion becomes more pronounced with increasing DMA concentrations (Fig. 1a). For example, chloride depletion decreased from 18.6 % to 13.5 % as DMA concentration increased from 50 to 150 ppb in the presence of NO_x (Exp.ND.1–ND.3). In the presence of SO_2 in Exp.SD.1–SD.3, it ranged from 12.1 % to 14.8 %, lower than that in Exp.S.1 (29.5 %). This is mainly because DMA, with a high vapor pressure, can react with inorganic acids (e.g., HNO_3, H_2SO_4, etc.) produced during the reaction to form aminium salts with lower vapor pressure (Wang et al., 2010; Murphy et al., 2007; Nielsen et al., 2012). Moreover, DMA can effectively promote cluster formation with H_2SO_4 or HNO_3, thereby generating DMA-H_2SO_4, DMA-H_2SO_4-H_2O clusters, and other nucleation systems (Chen et al., 2024a; Loukonen et al., 2010; Zhang et al., 2019). The aforementioned mechanisms can all reduce chloride depletion induced by inorganic acids.

As shown in Fig. 1a, chloride depletion in Exp.ND.2 (15.0 %) was lower than that in Exp.NA.1 (20.1 %). Similarly, it was lower (13.4 %) in Exp.SD.2 than in Exp.SA.1 (17.4 %). Despite the DMA concentration is lower than that of NH_3, chloride depletion in the presence of DMA (Exp.SD.1) was still weaker than that in the presence of NH_3 (Exp.SA.1). This can be attributed to DMA having a stronger alkalinity (Chen et al., 2022; Sauerwein and Chan, 2017; Xie et al., 2018), and a more effective nucleation ability (Ortega et al., 2012; Kupiainen et al., 2012) than NH_3. According to a theoretical study by Zhang et al. (2019), DMA is more likely than NH_3 to approach the air-nanoparticle interface, where the probability of its heterogeneous reaction with H_2SO_4 can increase. Notably, the neutralization efficiency of alkaline species can be affected by the particle phase state. When the phase state of particles changes from liquid to semisolid state, the neutralization efficiency of DMA may be relatively inhibited compared to that of the more mobile NH_3 (Sauerwein and Chan, 2017; DeRieux et al., 2019). The viscosity of SSA particles in our experiments was calculated to be 1.89–1.98 Pa s (details in the Supplement), being significantly lower than the 10^2 Pa s threshold for liquid-to-semisolid phase transition (DeRieux et al., 2018). This suggests that the SSA particles in this study existed in liquid state, and the neutralization efficiency of both ammonia and DMA was not constrained by phase transition.

Following the addition of isoprene, the weakening effect of DMA on chloride depletion in the presence of NO_x was not significantly different from that of experiments without isoprene. Nonetheless, this addition enhanced the weakening effect of DMA on chloride depletion in the presence of SO_2. Chloride depletion in Exp.ISD.2 was 3.8 %, significantly lower than that in Exp.SD.3 (12.1 %). This can be explained by the fact that organic acids produced from the oxidation of isoprene enhance DMA-H_2SO_4 nucleation, with a stronger enhancement effect observed at lower H_2SO_4 concentrations (Wang et al., 2022a; Lu et al., 2020). Isoprene oxidation products can react with H_2SO_4 to form organic sulfates (Armstrong et al., 2022; Wach et al., 2020), leading to a reduction in H_2SO_4 concentration within the reaction system.

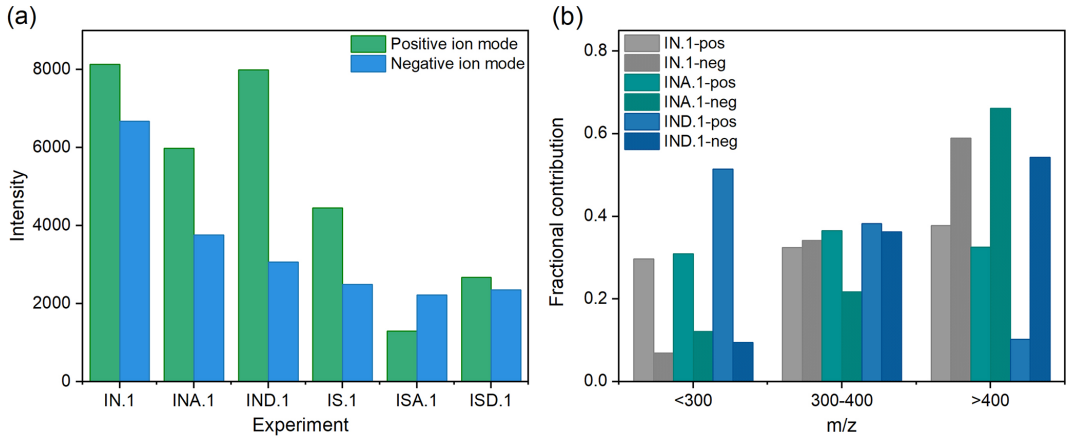

Figure 2. **(a)** Total signal intensity of identified organic chlorinated compounds for different experiments. **(b)** Distribution of identified molecules under different experimental conditions.

3.3 Formation of organic chlorinated compounds

The molecular composition of organic chlorinated compounds was analyzed, using UPLC/ESI-Q-TOF-MS, to further explore the effect of active chlorine on chloride depletion. Figure S3 presents the mass spectra of organic chlorinated compounds in the presence of acidic and alkaline gases. Mass spectra in both positive and negative ion modes contained numerous peaks, with compositions in the presence of NO_x being more complex than those in the presence of SO_2.

3.3.1 Effects of alkaline species in the presence of NO_x

As shown in Fig. 2a, the total signal intensity of the organic chlorinated compounds detected in the presence of alkaline species (Exp.INA.1 and Exp.IND.1) was lower than that in their absence (Exp.IN.1), indicating that the alkaline species reduce the formation of organic chlorinated compounds during the chloride depletion process. The identified organic chlorinated compounds were classified into three categories: $m/z < 300$, $300 \le m/z \le 400$ and $m/z > 400$ (Fig. 2b). The molecular weight distribution of products shifted with the addition of alkaline species. In the experiment without alkaline species (Exp.IN.1), molecules with high molecular weight ($m/z > 400$) had the highest proportion. In contrast, DMA reduced the proportion of high molecular weight molecules ($m/z > 400$), while increasing the intensity of molecules with m/z values in the ranges $m/z < 300$ and $300 \le m/z \le 400$ (Exp.IND.1) as shown in Fig. 2b. This suggests that the presence of DMA facilitates the formation of organic chlorinated compounds with lower molecular weight, which can be attributed to the stronger neutralization of the acidity by DMA, thereby inhibiting the acid-catalyzed polymerization reaction to generate high molecular weight molecules (Du et al., 2023). The lower proportion of organic chlorinated oligomers produced in Exp.IND.1 further supports this speculation (Fig. S4).

The Van Krevelen (VK) diagrams based on O/C and H/C ratios are presented in Fig. 3a–b. The H/C and O/C ratios of organic chlorinated compounds are primarily distributed in the ranges of 0.9–2.0 and 0.1–1.0. As shown in Fig. 3c, the organic chlorinated compounds produced in the presence of NH_3 (Exp.INA.1) exhibited the highest O/C ratio, which can be attributed to the presence of more hydroxyl, carbonyl, and carboxyl functional groups. The OS_C of organic chlorinated compounds in Exp.INA.1 was also higher, indicating that NH_3 enhances the degree of oxidation of organic chlorinated compounds (Fig. 3d). Conversely, the O/C ratio and OS_C of organic chlorinated compounds were low in the presence of DMA (Exp.IND.1). Figure S5 shows that the proportion of dichlorinated compounds in the presence of DMA is lower than that in the presence of NH_3, indicating that less active chlorine was produced in the presence of DMA and its multi-generation oxidation was inhibited. This result further supports that the weakening effect of DMA on chloride depletion is significantly more effective than that of NH_3 as mentioned above. Some organic chlorinated compounds (e.g., $C_5H_7ClO_4$, $C_8H_{11}ClO_5$, and $C_8H_{13}ClO_6$) detected in this study have also been reported in field observations (Chen et al., 2023), indicating that chloride depletion could be a source thereof in the ambient environment. These compounds were identified in our previous study and their formation pathways were proposed (Song et al., 2026).

As shown in Fig. S6, many unique molecules were detected in the experiments with alkaline species (Exp.INA.1 and Exp.IND.1), in addition to some compounds also detected in Exp.IN.1. In the experiment in the presence of NH_3 (Exp.INA.1), 42 and 30 unique molecules were detected in the positive and negative ion modes, respectively. When DMA was present (Exp.IND.1), 45 and 25 unique organic chlorinated compounds were identified in the pos-

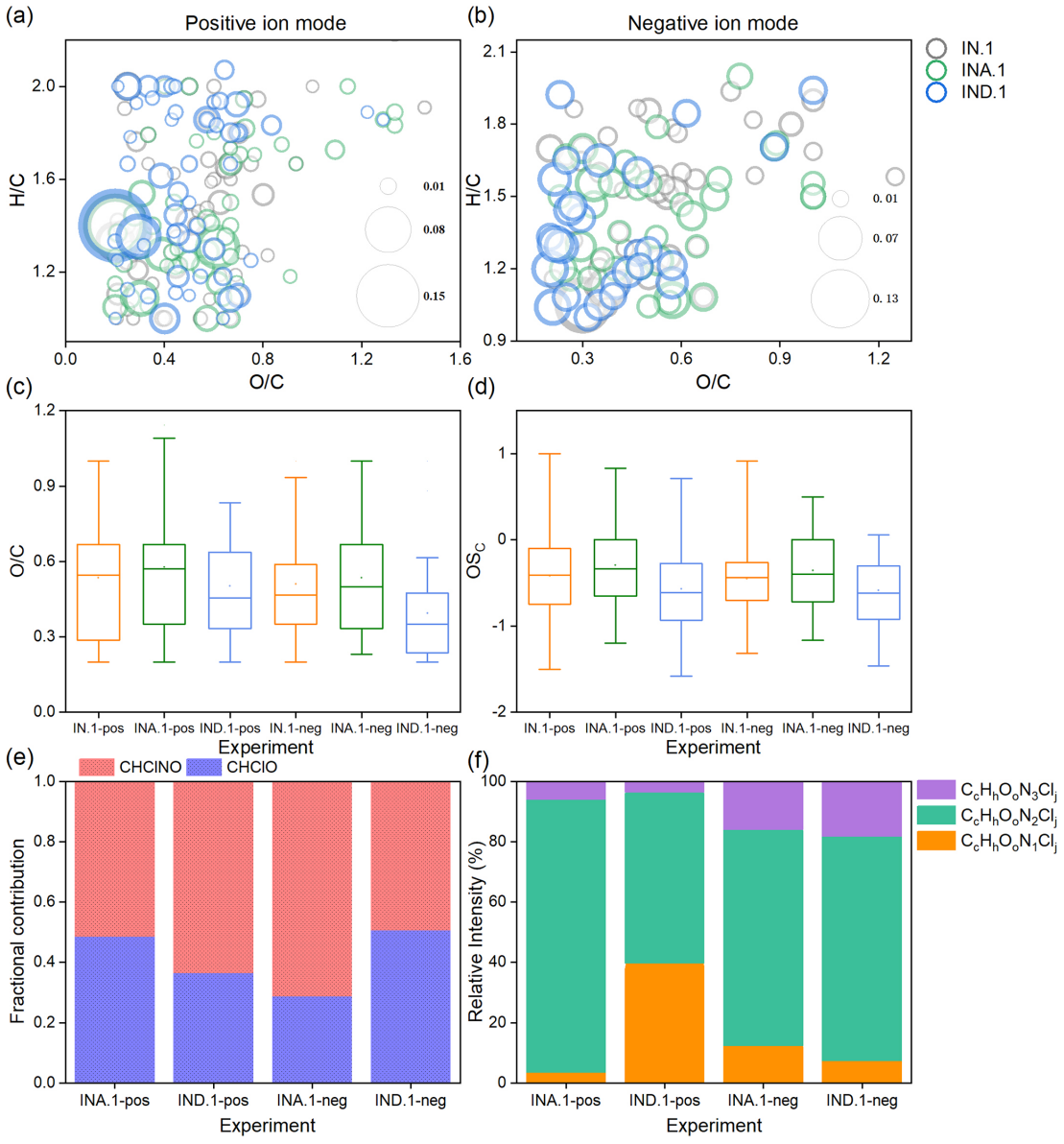

Figure 3. Van Krevelen diagram of organic chlorinated compounds for different experiments with NO_x in the **(a)** positive and **(b)** negative ion modes. The circle size represents the proportion of organic chlorinated compounds. **(c)** O/C and **(d)** OS_C of organic chlorinated compounds for different experiments with NO_x. **(e)** Fractional contribution to the total unique molecules by CHClO and CHClNO compounds in the presence of alkaline species. **(f)** Nitrogen atom distribution of CHClNO compounds in the presence of alkaline species for different experiments with NO_x.

itive and negative modes, respectively. These findings suggest that alkaline species alter the molecular composition of organic chlorinated compounds. The identified chlorinated species predominantly consisted of CHClO and CHClNO compounds, with the proportion of CHClNO being higher than that of CHClO (Fig. 3e). The CHClNO compounds primarily consist of N_2 products (Fig. 3f), and their formation is favored by high humidity (Yang et al., 2025). Representative CHClNO compounds include $C_9H_{14}ClNO_9$, $C_7H_{13}ClN_2O_4$, $C_6H_{10}ClNO_3$, etc. Figure 4 presents the formation mechanism of these compounds. Specifically, isoprene is oxidized by OH radicals to form key intermediates, which can be further oxidized by Cl radicals, yielding organic chlorinated monomers (e.g., $C_4H_5ClO_2$, $C_5H_9ClO_3$, $C_5H_9ClO_4$). These monomers can be converted into organic chlorinated oligomers through dehydration reactions or acid-catalyzed accretion reactions. Notably, NH_3 and DMA can react with these organic chlorinated compounds through acid-base neutralization to produce CHClNO compounds. For instance, NH_3 can react with $C_4H_8O_5$ to form $C_4H_{11}NO_5$. $C_4H_{11}NO_5$

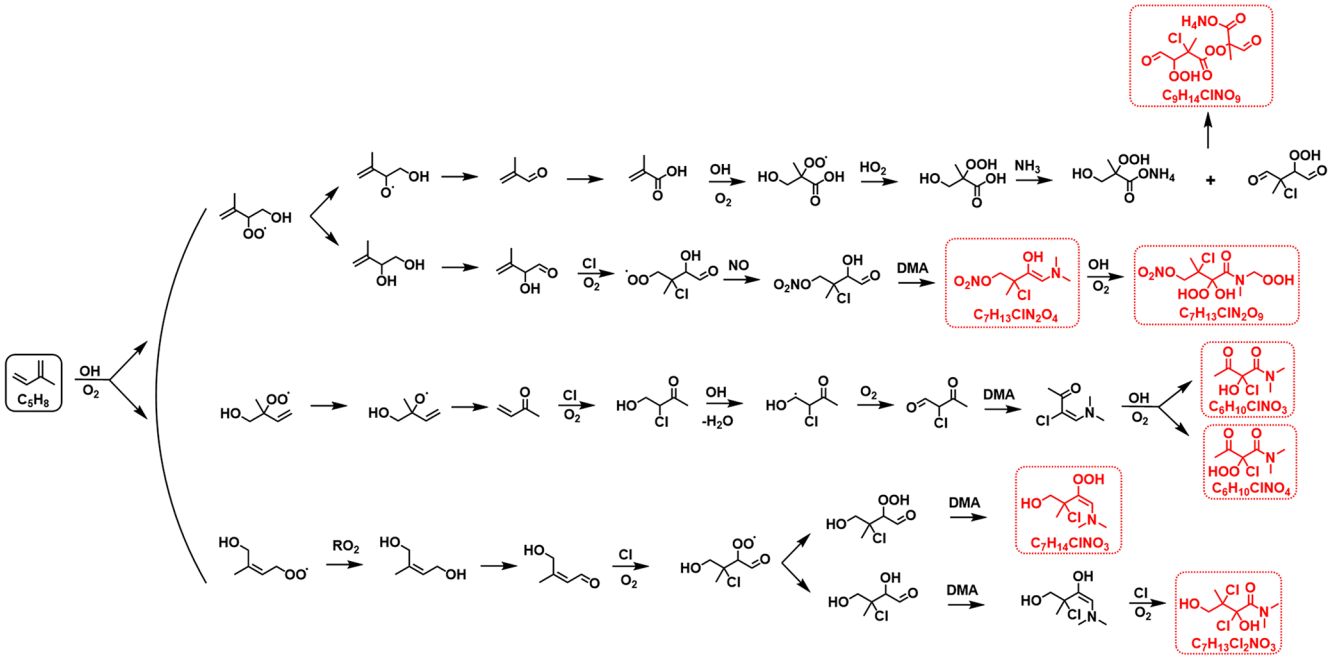

Figure 4. Formation mechanism of representative CHClNO compounds. The red boxes indicate the detected CHClNO compounds in our experiments.

and $C_5H_7ClO_4$ can undergo an accretion reaction to form $C_9H_{14}ClNO_9$. In addition, DMA can react with the aldehyde function of organic chlorinated compounds to form carbinolamines, which then dehydrate to form enamine compounds (e.g., $C_7H_{13}ClN_2O_4$ and $C_7H_{14}ClNO_2$). These enamine compounds can be further oxidized by OH and Cl radicals to produce the observed CHClNO compounds (e.g., $C_6H_{10}ClNO_3$, $C_7H_{13}Cl_2NO_3$, $C_7H_{13}ClN_2O_9$).

The toxicity prediction results of these organic chlorinated compounds are presented in Table S2. Results show that $C_7H_{13}ClN_2O_4$ compounds have the highest pLD_{50} values and are classified as class 3, indicating that they have considerable potential for acute toxicity. Notably, the predicted developmental toxicity values for the compounds listed in Table S2 have been classified as the highest hazard level, and they also pose mutagenicity risks. This highlights the necessity to conduct in-depth research on the toxicity of organic chlorinated compounds in the coastal atmosphere.

3.3.2 Effects of alkaline species in the presence of SO_2

In the presence of SO_2, the addition of NH_3 and DMA both significantly reduced the abundance of high molecular weight compounds (Fig. S7) and the total signal intensity of organic chlorinated compounds (Fig. 2a), which can be attributed to a reduced activation of chloride ions. This might be due to the fact that the addition of alkaline species reduces the production of gaseous HCl as a result of acid-base neutralization reactions and further diminishes the source of active chlorine (Edwards et al., 2024; Song et al., 2025). In addition, chloride ions can be activated into active chlorine by strong oxidants (OH radicals, O_3, etc.) (Zhang and Chan, 2023; Su et al., 2022). DMA can compete with chloride ions for these oxidants, thereby limiting the activation of chloride ions and reducing the generation of active chlorine species (Møller et al., 2020). The proportion of dichlorinated compounds in Exp.ISD.1 was significantly lower than that in Exp.IS.1 (Fig. 5a), mainly due to the reduction of active chlorine that inhibited its multi-generation oxidation. This further explains that the weakening effect of DMA on chloride depletion is enhanced in the presence of isoprene and SO_2.

As shown in Fig. 5b, in experiments with SO_2, the products detected in the positive ion mode mainly consisted of CHClO compounds, while the proportion of CHClSO compounds was the highest in the negative ion mode. This may be related to the different sensitivities of the compounds in different ion modes. CHClNO and CHClNSO compounds (including $C_7H_{15}ClN_2O_6$, $C_{13}H_{19}ClN_2O_6$, $C_{18}H_{35}ClN_2SO_8$, etc.) were also detected in experiments in the presence of alkaline species and SO_2. As mentioned above, the CHClNO compounds can be formed through the acid-base neutralization reaction or the reaction of DMA with aldehyde function. These compounds can react with H_2SO_4 through esterification reactions to form CHClNSO compounds. The observed higher proportion of CHClNO compounds in Exp.ISD.1 than that in Exp.ISA.1 (Fig. 5b) may result from the stronger ability of DMA to react with organic acids or carbonyl compounds (Smith et al., 2021). Moreover, autoxidation via a unimolecular reaction, being an important oxidation path-

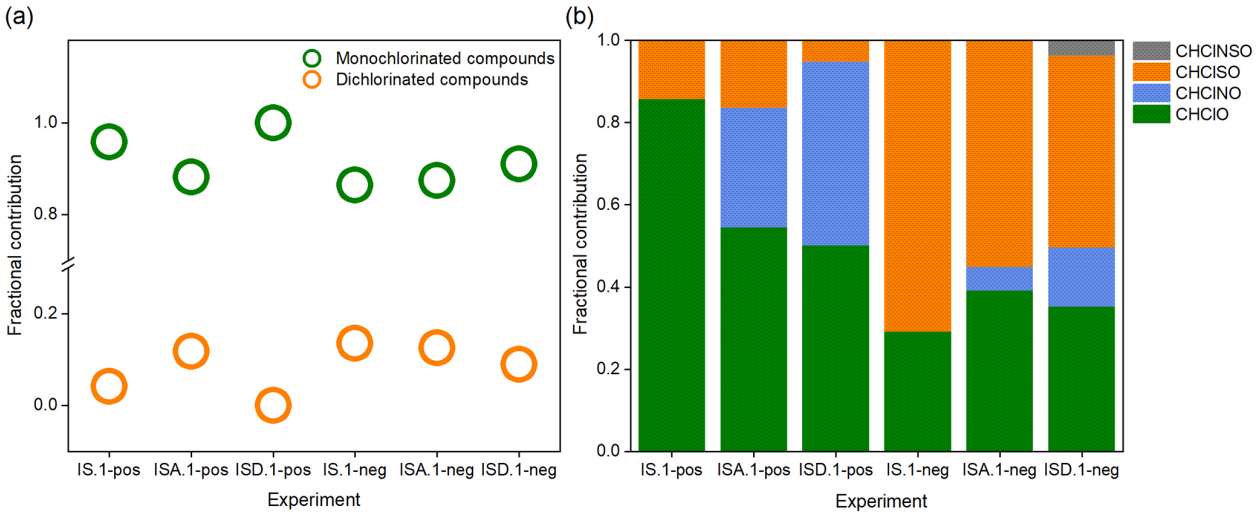

Figure 5. **(a)** Fractional contribution of monochlorinated and dichlorinated compounds in the total organic chlorinated compounds for different experiments with SO_2. **(b)** Fractional contribution to the total organic chlorinated compounds by different compounds.

way for DMA in the atmosphere, facilitates the formation of hydroperoxy amides (Møller et al., 2020). Overall, alkaline gases affect the formation of active chlorine during chloride depletion, and alters the composition of organic chlorinated compounds.

4 Conclusions

The complexity of atmospheric pollutants in coastal environments hinders the understanding of the mechanisms influencing chloride depletion. This study explored the detailed effects of NH_3 and DMA on this phenomenon. The results demonstrated that NH_3 and DMA could weaken the chloride depletion induced by acidic gases, with DMA exhibiting a more substantial weakening effect than NH_3. This difference in their impact is primarily due to DMA's stronger alkalinity and nucleation ability, which enable it to interact more effectively with acidic species than NH_3. Although the concentration of DMA in the atmosphere is lower than that of NH_3, its impact on chloride depletion is essential. The current results further reveal that considering only the effects of acidic gases may lead to deviations in the prediction of chloride depletion. This underscores the necessity to examine the role of alkaline species, especially organic amines, in future field studies of chloride depletion.

The mass spectrometry results showed that the presence of alkaline species also reduces the formation of organic chlorinated compounds, indicating that the generation of active chlorine is inhibited during chloride depletion. This can be attributed to the fact that the alkaline species reduce the generation of gaseous HCl through acid-base neutralization reactions, and can compete with chloride ions for oxidants, thereby further reducing the production of active chlorine. This further supports the idea that alkaline species could weaken the chloride depletion process. Additionally, the presence of alkaline species, especially DMA, promotes the formation of low-molecular-weight organic chlorinated compounds by neutralizing acidity, thereby inhibiting acid-catalyzed polymerization and the formation of high-molecular-weight compounds. The addition of alkaline species was observed to alter the composition of organic chlorinated compounds, with several identified unique products that were not present under acidic conditions. This suggests that alkaline species not only inhibit chloride depletion but also influence the overall chemical composition of the atmosphere by altering the chlorination pathways of organic compounds. The current results strengthen our understanding of the mechanism influencing chloride depletion, and provide a ground for the future identification of organic chlorinated compounds in ambient samples.

The initial concentrations of alkaline species used in the experiments were higher than the ambient levels. Moreover, the complex atmospheric chemical reactions were simplified in this study to eliminate the interference from other factors. Future studies should consider evaluating the effects of composition and phase state of aerosols on the mechanism and the extent of chloride depletion.

Data availability. Experimental data can be found at https://doi.org/10.5281/zenodo.18795123 (Song and Du, 2026).

Supplement. The supplement related to this article is available online at https://doi.org/10.5194/acp-26-6727-2026-supplement.

Author contributions. LD and AS designed the experiments, and AS carried them out. AS performed data analysis with assistance from LD, KL, and LX. AS wrote the paper with contributions from all co-authors, and co-authors commented on the paper.

Competing interests. The contact author has declared that none of the authors has any competing interests.

Disclaimer. Publisher's note: Copernicus Publications remains neutral with regard to jurisdictional claims made in the text, published maps, institutional affiliations, or any other geographical representation in this paper. The authors bear the ultimate responsibility for providing appropriate place names. Views expressed in the text are those of the authors and do not necessarily reflect the views of the publisher.

Acknowledgements. We thank Guannan Lin from the State Key Laboratory of Microbial Technology of Shandong University for help and guidance with UPLC/ESI-HR-Q-TOF-MS measurements.

Financial support. This work was supported by National Key Research and Development Program of China (2023YFC3706203), National Natural Science Foundation of China (U25A20787, 22376121), and Intramural Joint Program Fund of State Key Laboratory of Microbial Technology (SKLMTIJP-2025-02).

Review statement. This paper was edited by Bingbing Wang and reviewed by two anonymous referees.

References

Armstrong, N. C., Chen, Y., Cui, T., Zhang, Y., Christensen, C., Zhang, Z., Turpin, B. J., Chan, M. N., Gold, A., Ault, A. P., and Surratt, J. D.: Isoprene epoxydiol-derived sulfated and nonsulfated oligomers suppress particulate mass loss during oxidative aging of secondary organic aerosol, Environ. Sci. Technol., 56, 16611–16620, https://doi.org/10.1021/acs.est.2c03200, 2022.

Bates, K. H., Jacob, D. J., Cope, J. D., Chen, X., Millet, D. B., and Nguyen, T. B.: Emerging investigator series: Aqueous oxidation of isoprene-derived organic aerosol species as a source of atmospheric formic and acetic acids, Environ. Sci.-Atmos., 3, 1651–1664, https://doi.org/10.1039/d3ea00076a, 2023.

Behera, S. N. and Sharma, M.: Transformation of atmospheric ammonia and acid gases into components of $PM_{2.5}$: An environmental chamber study, Environ. Sci. Pollut. Res. 19, 1187–1197, https://doi.org/10.1007/s11356-011-0635-9, 2012.

Behera, S. N., Sharma, M., Aneja, V. P., and Balasubramanian, R.: Ammonia in the atmosphere: A review on emission sources, atmospheric chemistry and deposition on terrestrial bodies, Environ. Sci. Pollut. Res., 20, 8092–8131, https://doi.org/10.1007/s11356-013-2051-9, 2013.

Berner, A. H. and David Felix, J.: Investigating ammonia emissions in a coastal urban airshed using stable isotope techniques, Sci. Total Environ., 707, 134952, https://doi.org/10.1016/j.scitotenv.2019.134952, 2020.

Bian, Q., Huang, X. H. H., and Yu, J. Z.: One-year observations of size distribution characteristics of major aerosol constituents at a coastal receptor site in Hong Kong – Part 1: Inorganic ions and oxalate, Atmos. Chem. Phys., 14, 9013–9027, https://doi.org/10.5194/acp-14-9013-2014, 2014.

Braun, R. A., Dadashazar, H., MacDonald, A. B., Aldhaif, A. M., Maudlin, L. C., Crosbie, E., Aghdam, M. A., Hossein Mardi, A., and Sorooshian, A.: Impact of wildfire emissions on chloride and bromide depletion in marine aerosol particles, Environ. Sci. Technol., 51, 9013–9021, https://doi.org/10.1021/acs.est.7b02039, 2017.

Chen, D., Yao, X., Chan, C. K., Tian, X., Chu, Y., Clegg, S. L., Shen, Y., Gao, Y., and Gao, H.: Competitive uptake of dimethylamine and trimethylamine against ammonia on acidic particles in marine atmospheres, Environ. Sci. Technol., 56, 5430–5439, https://doi.org/10.1021/acs.est.1c08713, 2022.

Chen, D.-P., Ma, W., Yang, C.-H., Li, M., Zhou, Z.-Z., Zhang, Y., Wang, X.-C., and Quan, Z.-J.: Formation of atmospheric molecular clusters containing nitric acid with ammonia, methylamine, and dimethylamine, Environ. Sci.-Processes Impacts, 26, 2036–2050, https://doi.org/10.1039/d4em00330f, 2024a.

Chen, G., Xu, L., Yu, S., Xue, L., Lin, Z., Yang, C., Ji, X., Fan, X., Tham, Y. J., Wang, H., Hong, Y., Li, M., Seinfeld, J. H., and Chen, J.: Increasing contribution of chlorine chemistry to wintertime ozone formation promoted by enhanced nitrogen chemistry, Environ. Sci. Technol., 58, 22714–22721, https://doi.org/10.1021/acs.est.4c09523, 2024b.

Chen, H., Yan, C., Fu, Q., Wang, X., Tang, J., Jiang, B., Sun, H., Luan, T., Yang, Q., Zhao, Q., Li, J., Zhang, G., Zheng, M., Zhou, X., Chen, B., Du, L., Zhou, R., Zhou, T., and Xue, L.: Optical properties and molecular composition of wintertime atmospheric water-soluble organic carbon in different coastal cities of eastern China, Sci. Total Environ., 892, 164702, https://doi.org/10.1016/j.scitotenv.2023.164702, 2023.

Chen, W., Wang, X., Cohen, J. B., Zhou, S., Zhang, Z., Chang, M., and Chan, C.-Y.: Properties of aerosols and formation mechanisms over southern China during the monsoon season, Atmos. Chem. Phys., 16, 13271–13289, https://doi.org/10.5194/acp-16-13271-2016, 2016.

Dai, J., Wang, T., Shen, H., Xia, M., Sun, W., and Brasseur, G. P.: Significant impact of a daytime halogen oxidant on coastal air quality, Environ. Sci. Technol., 59, 2169–2180, https://doi.org/10.1021/acs.est.4c08360, 2025.

DeRieux, W.-S. W., Li, Y., Lin, P., Laskin, J., Laskin, A., Bertram, A. K., Nizkorodov, S. A., and Shiraiwa, M.: Predicting the glass transition temperature and viscosity of secondary organic material using molecular composition, Atmos. Chem. Phys., 18, 6331–6351, https://doi.org/10.5194/acp-18-6331-2018, 2018.

DeRieux, W.-S. W., Lakey, P. S. J., Chu, Y., Chan, C. K., Glicker, H. S., Smith, J. N., Zuend, A., and Shiraiwa, M.: Effects of phase state and phase separation on dimethylamine uptake of ammonium sulfate and ammonium sulfate-sucrose mixed particles, ACS Earth Space Chem., 3, 1268–1278, https://doi.org/10.1021/acsearthspacechem.9b00142, 2019.

Du, L., Xu, L., Li, K., George, C., and Ge, M.: NH_3 weakens the enhancing effect of SO_2 on biogenic secondary organic

aerosol formation, Environ. Sci. Technol. Let., 10, 145–151, https://doi.org/10.1021/acs.estlett.2c00959, 2023.

Du, W., Wang, X., Yang, F., Bai, K., Wu, C., Liu, S., Wang, F., Lv, S., Chen, Y., Wang, J., Liu, W., Wang, L., Chen, X., and Wang, G.: Particulate amines in the background atmosphere of the Yangtze River Delta, China: Concentration, size distribution, and sources, Adv. Atmos. Sci., 38, 1128–1140, https://doi.org/10.1007/s00376-021-0274-0, 2021.

Duan, Y., Liu, Y., Zhang, K., Li, L., Huo, J., Chen, J., Fu, Q., Gao, Z., Xiu, G., and Hu, T.: Variations of chloride depletion and its impacts on ozone formation: Case study of a coastal area in Shanghai, Sci. Total Environ., 957, 176899, https://doi.org/10.1016/j.scitotenv.2024.176899, 2024.

Edwards, E.-L., Choi, Y., Crosbie, E. C., DiGangi, J. P., Diskin, G. S., Robinson, C. E., Shook, M. A., Winstead, E. L., Ziemba, L. D., and Sorooshian, A.: Sea salt reactivity over the northwest Atlantic: an in-depth look using the airborne ACTIVATE dataset, Atmos. Chem. Phys., 24, 3349–3378, https://doi.org/10.5194/acp-24-3349-2024, 2024.

Ghosh, A., Roy, A., Das, S. K., Ghosh, S. K., Raha, S., and Chatterjee, A.: Identification of most preferable reaction pathways for chloride depletion from size segregated sea-salt aerosols: A study over high altitude Himalaya, tropical urban metropolis and tropical coastal mangrove forest in eastern India, Chemosphere, 245, 125673, https://doi.org/10.1016/j.chemosphere.2019.125673, 2020.

Hoffmann, E. H., Tilgner, A., Wolke, R., and Herrmann, H.: Enhanced chlorine and bromine atom activation by hydrolysis of halogen nitrates from marine aerosols at polluted coastal areas, Environ. Sci. Technol., 53, 771–778, https://doi.org/10.1021/acs.est.8b05165, 2019.

Jenkin, M. E., Young, J. C., and Rickard, A. R.: The MCM v3.3.1 degradation scheme for isoprene, Atmos. Chem. Phys., 15, 11433–11459, https://doi.org/10.5194/acp-15-11433-2015, 2015.

Kupiainen, O., Ortega, I. K., Kurtén, T., and Vehkamäki, H.: Amine substitution into sulfuric acid – ammonia clusters, Atmos. Chem. Phys., 12, 3591–3599, https://doi.org/10.5194/acp-12-3591-2012, 2012.

Lan, Z., Lin, W., and Zhao, G.: Sources, variations, and effects on air quality of atmospheric ammonia, Curr. Pollution Rep., 10, 40–53, https://doi.org/10.1007/s40726-023-00291-6, 2024.

Li, X., Jia, L., Xu, Y., and Pan, Y.: A novel reaction between ammonia and Criegee intermediates can form amines and suppress oligomers from isoprene, Sci. Total Environ., 956, 177389, https://doi.org/10.1016/j.scitotenv.2024.177389, 2024.

Liu, M., Wang, X., Liu, Z., Jiang, Y., Li, M., Zhang, J., Sun, Y., Zhu, Y., Xue, L., and Wang, W.: Characteristics and origins of fine particulate amines at a coastal mountain site in northern China in spring, Atmos. Environ., 321, https://doi.org/10.1016/j.atmosenv.2024.120365, 2024a.

Liu, M., Wang, X., Liu, Z., Jiang, Y., Li, M., Zhang, J., Sun, Y., Zhu, Y., Xue, L., and Wang, W.: Characteristics and origins of fine particulate amines at a coastal mountain site in northern China in spring, Atmos. Environ., 321, 120365, https://doi.org/10.1016/j.atmosenv.2024.120365, 2024b.

Liu, T., Xu, Y., Sun, Q. B., Xiao, H. W., Zhu, R. G., Li, C. X., Li, Z. Y., Zhang, K. Q., Sun, C. X., and Xiao, H. Y.: Characteristics, origins, and atmospheric processes of amines in fine aerosol particles in winter in China, J. Geophys. Res.-Atmos., 128, e2023JD038974, https://doi.org/10.1029/2023jd038974, 2023.

Liu, X., Liu, L., Zhang, B., Liu, P., Huang, R.-J., Hildebrandt Ruiz, L., Miao, R., Chen, Q., and Wang, X.: Modeling the global impact of chlorine chemistry on secondary organic aerosols, Environ. Sci. Technol., 58, 23064–23074, https://doi.org/10.1021/acs.est.4c05037, 2024c.

Liu, Z., Li, M., Wang, X., Liang, Y., Jiang, Y., Chen, J., Mu, J., Zhu, Y., Meng, H., Yang, L., Hou, K., Wang, Y., and Xue, L.: Large contributions of anthropogenic sources to amines in fine particles at a coastal area in northern China in winter, Sci. Total Environ., 839, 156281, https://doi.org/10.1016/j.scitotenv.2022.156281, 2022.

Loukonen, V., Kurtén, T., Ortega, I. K., Vehkamäki, H., Pádua, A. A. H., Sellegri, K., and Kulmala, M.: Enhancing effect of dimethylamine in sulfuric acid nucleation in the presence of water – a computational study, Atmos. Chem. Phys., 10, 4961–4974, https://doi.org/10.5194/acp-10-4961-2010, 2010.

Lu, Y., Liu, L., Ning, A., Yang, G., Liu, Y., Kurtén, T., Vehkamäki, H., Zhang, X., and Wang, L.: Atmospheric sulfuric acid-dimethylamine nucleation enhanced by trifluoroacetic acid, Geophys. Res. Lett., 47, e2019GL085627, https://doi.org/10.1029/2019gl085627, 2020.

Møller, K. H., Berndt, T., and Kjaergaard, H. G.: Atmospheric autoxidation of amines, Environ. Sci. Technol., 54, 11087–11099, https://doi.org/10.1021/acs.est.0c03937, 2020.

Murphy, S. M., Sorooshian, A., Kroll, J. H., Ng, N. L., Chhabra, P., Tong, C., Surratt, J. D., Knipping, E., Flagan, R. C., and Seinfeld, J. H.: Secondary aerosol formation from atmospheric reactions of aliphatic amines, Atmos. Chem. Phys., 7, 2313–2337, https://doi.org/10.5194/acp-7-2313-2007, 2007.

Nielsen, C. J., Herrmann, H., and Weller, C.: Atmospheric chemistry and environmental impact of the use of amines in carbon capture and storage (CCS), Chem. Soc. Rev., 41, 6684–6704, https://doi.org/10.1039/c2cs35059a, 2012.

Nolte, C., Bhave, P., Arnold, J., Dennis, R., Zhang, K., and Wexler, A.: Modeling urban and regional aerosols-Application of the CMAQ-UCD aerosol model to Tampa, a coastal urban site, Atmos. Environ., 42, 3179–3191, https://doi.org/10.1016/j.atmosenv.2007.12.059, 2008.

Nolte, C. G., Appel, K. W., Kelly, J. T., Bhave, P. V., Fahey, K. M., Collett Jr., J. L., Zhang, L., and Young, J. O.: Evaluation of the Community Multiscale Air Quality (CMAQ) model v5.0 against size-resolved measurements of inorganic particle composition across sites in North America, Geosci. Model Dev., 8, 2877–2892, https://doi.org/10.5194/gmd-8-2877-2015, 2015.

Ortega, I. K., Kupiainen, O., Kurtén, T., Olenius, T., Wilkman, O., McGrath, M. J., Loukonen, V., and Vehkamäki, H.: From quantum chemical formation free energies to evaporation rates, Atmos. Chem. Phys., 12, 225–235, https://doi.org/10.5194/acp-12-225-2012, 2012.

Rankin, A. M. and Wolff, E. W.: A year-long record of size-segregated aerosol composition at Halley, Antarctica, J. Geophys. Res.-Atmos., 108, 4775, https://doi.org/10.1029/2003jd003993, 2003.

Sauerwein, M. and Chan, C. K.: Heterogeneous uptake of ammonia and dimethylamine into sulfuric and oxalic acid particles, Atmos. Chem. Phys., 17, 6323–6339, https://doi.org/10.5194/acp-17-6323-2017, 2017.

Smith, A. M., Keene, W. C., Maben, J. R., Pszenny, A. A. P., Fischer, E., and Stohl, A.: Ammonia sources, transport, transformation, and deposition in coastal New England during summer, J. Geophys. Res.-Atmos., 112, https://doi.org/10.1029/2006jd007574, 2007.

Smith, N. R., Montoya-Aguilera, J., Dabdub, D., and Nizkorodov, S. A.: Effect of humidity on the reactive uptake of ammonia and dimethylamine by nitrogen-containing secondary organic aerosol, Atmosphere, 12, https://doi.org/10.3390/atmos12111502, 2021.

Song, A. and Du, L.: Organic amine weakens chloride depletion in coastal atmosphere, Zenodo [data set], https://doi.org/10.5281/zenodo.18795123, 2026.

Song, A., Li, K., Yang, Z., Tsona Tchinda, N., and Du, L.: Marine volatile organic compounds promote the chloride depletion in sea salt aerosols, J. Geophys. Res. Atmos., 130, e2025JD043495, https://doi.org/10.1029/2025JD043495, 2025.

Song, A., Li, K., Yang, Z., Xu, L., Chen, X., Tsona Tchinda, N., and Du, L.: Anthropogenic-biogenic interaction drives chloride depletion in coastal atmospheres, Environ. Sci. Technol., https://doi.org/10.1021/acs.est.6c02035, 2026.

Su, B., Wang, T., Zhang, G., Liang, Y., Lv, C., Hu, Y., Li, L., Zhou, Z., Wang, X., and Bi, X.: A review of atmospheric aging of sea spray aerosols: Potential factors affecting chloride depletion, Atmos. Environ., 290, 119365, https://doi.org/10.1016/j.atmosenv.2022.119365, 2022.

Wach, P., Spólnik, G., Surratt, J. D., Blaziak, K., Rudzinski, K. J., Lin, Y.-H., Maenhaut, W., Danikiewicz, W., Claeys, M., and Szmigielski, R.: Structural characterization of lactone-containing MW 212 organosulfates originating from isoprene oxidation in ambient fine aerosol, Environ. Sci. Technol., 54, 1415–1424, https://doi.org/10.1021/acs.est.9b06190, 2020.

Wang, C., Liu, Y., Huang, T., Feng, Y., Wang, Z., Lu, R., and Jiang, S.: Sulfuric acid-dimethylamine particle formation enhanced by functional organic acids: An integrated experimental and theoretical study, Phys. Chem. Chem. Phys., 24, 23540–23550, https://doi.org/10.1039/d2cp01671k, 2022a.

Wang, D. S., Masoud, C. G., Modi, M., and Hildebrandt Ruiz, L.: Isoprene-chlorine oxidation in the presence of NO_x and implications for urban atmospheric chemistry, Environ. Sci. Technol., 56, 9251–9264, https://doi.org/10.1021/acs.est.1c07048, 2022b.

Wang, L., Lal, V., Khalizov, A. F., and Zhang, R.: Heterogeneous chemistry of alkylamines with sulfuric acid implications for atmospheric formation-of alkylaminium sulfates, Environ. Sci. Technol., 44, 2461–2465, https://doi.org/10.1021/es9036868, 2010.

Wang, M., Kong, W., Marten, R., He, X.-C., Chen, D., Pfeifer, J., Heitto, A., Kontkanen, J., Dada, L., Kürten, A., Yli-Juuti, T., Manninen, H. E., Amanatidis, S., Amorim, A., Baalbaki, R., Baccarini, A., Bell, D. M., Bertozzi, B., Bräkling, S., Brilke, S., Murillo, L. C., Chiu, R., Chu, B., De Menezes, L.-P., Duplissy, J., Finkenzeller, H., Carracedo, L. G., Granzin, M., Guida, R., Hansel, A., Hofbauer, V., Krechmer, J., Lehtipalo, K., Lamkaddam, H., Lampimäki, M., Lee, C. P., Makhmutov, V., Marie, G., Mathot, S., Mauldin, R. L., Mentler, B., Müller, T., Onnela, A., Partoll, E., Petäjä, T., Philippov, M., Pospisilova, V., Ranjithkumar, A., Rissanen, M., Rörup, B., Scholz, W., Shen, J., Simon, M., Sipilä, M., Steiner, G., Stolzenburg, D., Tham, Y. J., Tomé, A., Wagner, A. C., Wang, D. S., Wang, Y., Weber, S. K., Winkler, P. M., Wlasits, P. J., Wu, Y., Xiao, M., Ye, Q., Zauner-Wieczorek, M., Zhou, X., Volkamer, R., Riipinen, I., Dommen, J., Curtius, J., Baltensperger, U., Kulmala, M., Worsnop, D. R., Kirkby, J., Seinfeld, J. H., El-Haddad, I., Flagan, R. C., and Donahue, N. M.: Rapid growth of new atmospheric particles by nitric acid and ammonia condensation, Nature, 581, 184–189, https://doi.org/10.1038/s41586-020-2270-4, 2020.

Wennberg, P. O., Bates, K. H., Crounse, J. D., Dodson, L. G., McVay, R. C., Mertens, L. A., Nguyen, T. B., Praske, E., Schwantes, R. H., Smarte, M. D., St Clair, J. M., Teng, A. P., Zhang, X., and Seinfeld, J. H.: Gas-phase reactions of isoprene and its major oxidation products, Chem. Rev., 118, 3337–3390, https://doi.org/10.1021/acs.chemrev.7b00439, 2018.

Wolfe, G. M., Marvin, M. R., Roberts, S. J., Travis, K. R., and Liao, J.: The Framework for 0-D Atmospheric Modeling (F0AM) v3.1, Geosci. Model Dev., 9, 3309–3319, https://doi.org/10.5194/gmd-9-3309-2016, 2016.

Wu, K., Zhu, S., Liu, Y., Wang, H., Yang, X., Liu, L., Dabdub, D., and Cappa, C. D.: Modeling ammonia and its uptake by secondary organic aerosol over China, J. Geophys. Res.-Atmos., 126, e2020JD034109, https://doi.org/10.1029/2020jd034109, 2021.

Xie, H., Feng, L., Hu, Q., Zhu, Y., Gao, H., Gao, Y., and Yao, X.: Concentration and size distribution of water-extracted dimethylaminium and trimethylaminium in atmospheric particles during nine campaigns – Implications for sources, phase states and formation pathways, Sci. Total Environ., 631–632, 130–141, https://doi.org/10.1016/j.scitotenv.2018.02.303, 2018.

Xu, L., Liu, X., Gao, H., Yao, X., Zhang, D., Bi, L., Liu, L., Zhang, J., Zhang, Y., Wang, Y., Yuan, Q., and Li, W.: Long-range transport of anthropogenic air pollutants into the marine air: insight into fine particle transport and chloride depletion on sea salts, Atmos. Chem. Phys., 21, 17715–17726, https://doi.org/10.5194/acp-21-17715-2021, 2021.

Yang, Z., Li, K., and Du, L.: Highly oxidized molecules make a significant contribution to enhanced aromatic-derived secondary organic aerosol under a humid environment, Adv. Atmos. Sci., 42, 641–652, https://doi.org/10.1007/s00376-024-4085-y, 2025.

Yao, X., Fang, M., and Chan, C. K.: The size dependence of chloride depletion in fine and coarse sea-salt particles, Atmos. Environ., 37, 743–751, https://doi.org/10.1016/S1352-2310(02)00955-X, 2003.

Yu, Z. and Li, Y.: Marine volatile organic compounds and their impacts on marine aerosol – A review, Sci. Total Environ., 768, 145054, https://doi.org/10.1016/j.scitotenv.2021.145054, 2021.

Zhan, J., Li, W., Chen, L., Lin, Q., and Gao, Y.: Anthropogenic influences on aerosols at Ny-Ålesund in the summer Arctic, Atmos. Pollut. Res., 8, 383–393, https://doi.org/10.1016/j.apr.2016.10.010, 2017.

Zhang, R. and Chan, C. K.: Simultaneous formation of sulfate and nitrate via co-uptake of SO_2 and NO_2 by aqueous NaCl droplets: combined effect of nitrate photolysis and chlorine chemistry, Atmos. Chem. Phys., 23, 6113–6126, https://doi.org/10.5194/acp-23-6113-2023, 2023.

Zhang, W., Ji, Y., Li, G., Shi, Q., and An, T.: The heterogeneous reaction of dimethylamine/ammonia with sulfuric acid to promote the growth of atmospheric nanoparticles, Environ. Sci.-Nano, 6, 2767–2776, https://doi.org/10.1039/c9en00619b, 2019.

Zhang, W., Weber, J., Archibald, A. T., Abraham, N. L., Booge, D., Yang, M., and Gu, D.: Global atmospheric composition effects from marine isoprene emissions, Environ. Sci. Technol., 59, 2554–2564, https://doi.org/10.1021/acs.est.4c10657, 2025.

Zhou, S., Salter, M., Bertram, T., Brito Azevedo, E., Reis, F., and Wang, J.: Shoreline wave breaking strongly enhances the coastal sea spray aerosol population: Climate and air quality implications, Sci. Adv., 11, eadw0343, https://doi.org/10.1126/sciadv.adw0343, 2025.

Zou, Z., Chen, Q., Xia, M., Yuan, Q., Chen, Y., Wang, Y., Xiong, E., Wang, Z., and Wang, T.: OH measurements in the coastal atmosphere of South China: possible missing OH sinks in aged air masses, Atmos. Chem. Phys., 23, 7057–7074, https://doi.org/10.5194/acp-23-7057-2023, 2023.